Coster-Kronig Decay of the Ar 2*s* Hole Observed by Auger-Threshold Photoelectron Coincidence Spectroscopy

P. Lablanquie,[1] F. Penent,[2] R. I. Hall,[2] H. Kjeldsen,[3] J. H. D. Eland,[4] A. Muehleisen,[5] P. Pelicon,[5] Ž. Šmit,[5] M. Žitnik, and F. Koike[6]

[1]*L.U.R.E. Centre Universitaire Paris-Sud, Bâtiment 209D, BP 34, 91898 Orsay Cedex, France*
[2]*D.I.A.M., Université P. & M. Curie, 4 pl. Jussieu, 75252 Paris 5, France*
[3]*Institute for Physics and Astronomy, University of Aarhus, 8000 Aarhus, Denmark*
[4]*Physical and Theoretical Chemistry Laboratory, Oxford OX1 3QZ, United Kingdom*
[5]*Institute J. Stefan, Jamova 39, 1000 Ljubljana, Slovenia*
[6]*School of Medicine, Kitasato University, Sagamihara 228, Japan*

(Received 20 January 1999)

The Coster-Kronig lines associated with Ar 2*s* decay have been resolved within the natural linewidth of the 2*s* hole for the first time. This was possible by a new spectroscopic technique, relying on resonance enhanced double photoionization, Auger-threshold photoelectron coincidence spectroscopy. Contrary to standard Auger spectroscopy, this technique can filter out weak components in Auger spectra corresponding to a well-defined inner-shell state and, furthermore, can achieve a resolution no longer limited by the lifetime of the inner-shell hole.

PACS numbers: 32.80.Fb, 07.81.+a, 32.80.Hd

Auger spectroscopy has become a powerful analytical tool, especially in the field of surface and solid state physics, as Auger lines are characteristic not only of the emitting atom but also of its environment. However, detailed understanding of Auger spectra is still limited, for two main reasons. First, the spectra contain a complex superposition of components associated with a range of different initial inner-shell states. Second, the resolution with which one can observe Auger spectra or resonant Auger spectra is normally limited by the natural width corresponding to the lifetime τ of these hole states. These limitations can be overcome by using monochromatized synchrotron light to form the initial hole state and by measuring the Auger spectra in coincidence with the associated photoelectrons. Energy selection of the photoelectron identifies a single initial hole state; measurement of the coincident Auger electron energy fixes the final state energy, avoiding the resolution limitation due to the natural lifetime of the intermediate state [1]. This has been implemented in a new technique, "Auger-threshold photoelectron coincidence spectroscopy," where the photoelectrons have near-zero energy and are formed when the photon energy is equal to the threshold energy of an ionization process. This technique has inherent high efficiency and resolution as threshold electrons can be detected over 4π sr with a resolution in the meV range. Herein, we demonstrate the power of this method by detecting and resolving the structure of the weak Coster-Kronig Auger lines associated with the Ar 2*s* hole, masked until now by the large natural width, $\Gamma = 1/\tau$, of the 2*s* hole [2], measured to be 2.25 ± 0.05 eV [3].

The use of electron-electron coincidence techniques in atomic and molecular physics to disentangle the complexity of Auger spectra has remained quite limited [4–7]. It is in the field of solid state and surface physics that Auger-photoelectron coincidence spectroscopy (APECS) has the longest history as a tool for sorting out Auger emission spectra from transition materials [8]. Although the possibility of achieving a spectroscopic resolution which is no longer limited by the lifetime of the inner-shell hole was mentioned in APECS studies, the first experimental demonstration was given only recently by Viefhaus *et al.* [1] in their study of Xe 4*d* decay. The Auger process following photoabsorption can be written as

$$h\nu + A \rightarrow A^{+}(nl^{-1}) + e_{\text{photoel}} \rightarrow A^{++} + e_{\text{Auger}} + e_{\text{photoel}}\,. \quad (1)$$

It is then obvious that the law of conservation of energy between the initial and final states of the system,

$$h\nu = \text{binding } E(A^{++}) + \text{kinetic } E(e_{\text{Auger}}) + \text{kinetic } E(e_{\text{photoel}})\,, \quad (2)$$

suffers no constraints from the intermediate state. Thus, the achievable resolution when the energies of the two electrons are measured simultaneously depends on the instrumental performance alone and is limited only by the lifetime width of the final A^{++} state (usually small), and not by that of the intermediate A^{+} (nl^{-1}) state.

The experiments were performed on beam line SA72 at the SuperACO storage ring in Orsay, France. This beam line is equipped with a plane grating; its best resolution is about 250 meV at the Ar 2*p* edge, and was degraded to 650 meV in these experiments to increase the coincidence signal. The light beam crosses, at right angles, the target gas beam effusing from a hypodermic needle. Threshold photoelectrons are detected by a threshold photoelectron spectrometer [9] that uses the penetrating field technique [10]. Auger electrons are detected in a 55 cm time-of-flight (TOF) analyzer, based on those developed by Langer *et al.* ([11], and references

therein), mounted parallel to the electric field vector of the photons. Coincidences between the Auger and threshold electrons were recorded in the two-bunch operating mode of the storage ring that permits precise measurement (± 1 ns) of the Auger electron flight time and energy (± 0.2 eV at 50 eV).

Figure 1 shows the yield of threshold electrons as a function of photon energy, in the vicinity of the Ar L shell edges. This spectrum reveals structure due to excitation and ionization associated with $2p$, $2pnl$ satellite, and $2s$ holes. The structure observed here has been much studied previously ([12], and references therein). Note that, in a threshold spectrum, the ionization peaks are shifted from their nominal binding energy by postcollision interaction (PCI). The $2s$ peak maximum, for instance, lies at 327.5 eV compared to a binding energy of 326.25 eV [3]. Coincidences between the $2s$ threshold photoelectrons and the associated Auger lines were recorded with the photon energy set at the maximum of the $2s$ peak. The resulting time-of-flight spectrum set on energy scales is displayed in Fig. 2(a). This figure shows the Ar^{++} $2p^{-1}3p^{-1}$ states formed by the $L_1L_{2,3}M_{2,3}$ Coster-Kronig transitions. Comparison with the "noncoincident" Auger spectrum of Mehlhorn [2] demonstrates, as expected, the absence of broadening due to the $2s$ hole lifetime. The total experimental resolution amounts to 650 meV and is exclusively determined by the photons.

In order to assign the peaks in Fig. 2(a), calculations of the Ar $L_1L_{2,3}M_{2,3}$ transitions were performed. The Auger transition energies were calculated according to atomic state functions (ASF); the spectroscopic notations are representative of only the largest contribution to a particular ASF. The intensities were obtained using a modified GRASP program package with Dirac-Fock continuum wave functions. A set of bound radial wave functions was calculated in the potential of the final atomic configuration Ar^{++} $2p^{-1}3p^{-1}$ and of the initial atomic configuration Ar^{++} $2s^{-1}$. Continuum wave functions were then calculated using the final atomic core configuration. The calculated energies (shifted down by 2.9 eV) and intensities are listed in Table I and displayed in Fig. 2(b). The agreement with the present observations and with those of Mehlhorn [2] is generally good, thus allowing the assignment of the coincident Auger lines. There appears to be a discrepancy in the ^1S relative intensity. This could be due to the experimental difficulty in correcting the transmission function of the TOF

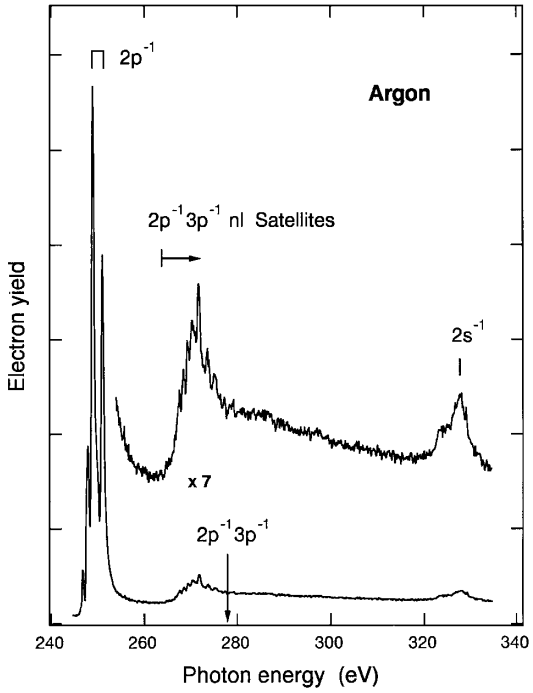

FIG. 1. Yield of threshold electrons against photon energy.

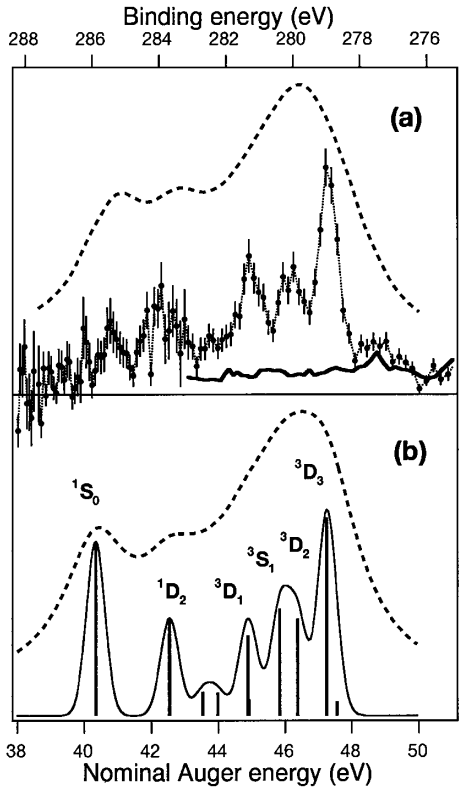

FIG. 2. (a) $L_1L_{2,3}M_{2,3}$ Coster-Kronig lines measured in coincidences with $2s$ photoelectrons at $h\nu = 327.5$ eV, compared with the noncoincident Auger spectrum from [2] (dashed line). The "nominal" Auger electron energy corresponds to the measured coincident Auger electron energy corrected for the PCI shift, Δ(PCI), where $\Delta(\mathrm{PCI}) = h\nu - \text{binding } E(\mathrm{Ar}^+\ 2s)$. The binding energy scale of the Ar^{++} final states follows (2). The solid line represents the estimated contribution of double and cascade Auger processes (see text). The accumulation time was 6 h. Intensities have been corrected by the Jacobian of the time-to-energy scale transformation, as well as by the transmission function of the spectrometer. (b) This shows the theoretical calculations from Table I, column A (sticks) convoluted with a 650 meV Gaussian function corresponding to the experimental resolution (solid line), and convoluted with a 2.25 eV Lorentzian function corresponding to the noncoincident Auger spectrum (dashed line).

TABLE I. Ar $L_1L_{2,3}M_{2,3}$ Coster-Kronig lines: comparison of experimental and calculated energies. Column A: Ar^{++} $2p^{-1}3p^{-1}$ potential was used in the calculation of bound radial wave functions. Column B: Ar^{+} $2s^{-1}$ potential was used. Column C: results summed over J.

Final state assignment	Calculated intensity (a.u. $\times 10^{-3}$)			Calculated energy (eV)	Experimental energy (eV)	Calculated energy[a] (eV)
	A	B	C[b]			
$^1P_1$	0.83	1.08	⋯	47.56	⋯	47.56
$^3D_3$	11.7	17.9	36.11	47.25	47.3 ± 0.2	47.26
$^3D_2$	5.75	9.01	⋯	46.37	⋯	46.41
$^3S_1$	6.33	6.64	8.52	45.84	46.15 ± 0.2	45.91
$^3P_2$	0.97	1.52	⋯	44.92	⋯	45.10
$^3D_1$	4.75	5.43	⋯	44.89	45.0 ± 0.2	45.00
$^3P_0$	1.35	1.41	⋯	43.98	⋯	44.28
$^3P_1$	1.41	1.61	⋯	43.53	⋯	43.77
$^1D_2$	5.75	9.32	17.23	42.55	42.35 ± 0.2	43.0
$^1S_0$	10.3	10.8	15.36	40.34	40.9 ± 0.2	41.14
Sum	49.2	64.7	77.22			

[a]Mehlhorn [2].
[b]Karim and Crasemann [13].

analyzer in this part of the spectrum corresponding to the lowest energy electrons. On the theoretical side, the sudden model was used and the effect of relaxation of the atom during the Auger transition, as well as insufficient configurations in the calculations, could modify the relative line intensities. It seems that channel coupling does not substantially change these intensities as shown by the results of Karim and Crasemann [13] (Table I, column C). Note that the measured intensities are not affected by the angular distribution because the noncoincident angular distribution of $L_1L_{2,3}M_{2,3}$ Auger electrons is expected to be isotropic as the alignment of the initial hole with total angular momentum $j = \frac{1}{2}$ is zero [14]. The same holds for the angular distribution of the coincidence signal as the threshold electrons were collected over 4π sr.

As can be seen in Fig. 1, the $2s$ peak represents only about one-third of the total threshold electron intensity, and the coincident spectrum in Fig. 2(a) also contains contributions from the threshold electrons which are not associated with the $2s$ hole. In coincident spectra measured in the case of Xe $4d$ ionization [15], it was observed that double Auger, i.e., simultaneous emission of two electrons which randomly share the available energy, and/or cascade Auger transitions can result in the emission of threshold Auger electrons. These processes explain the general increase in yield of threshold electrons above each ionization edge as well as the intensity beneath the $2s$ structure of Fig. 1. The contribution here from coincidences between these threshold Auger electrons and what are most probably $2p$ satellite photoelectrons has been estimated by comparison with a noncoincident spectrum and is shown in Figs. 2(a) and 3(b) (solid lines).

Figure 3 shows coincident spectra taken above and below the Ar $2s$ threshold compared to that recorded on the $2s$ peak. The above-mentioned structure associated with Auger threshold electrons and the $2p$ satellites keeps a fairly constant intensity in the three spectra. But what is of particular interest is the coincidence signal at the Coster-Kronig line positions even when the $2s$ photoelectron is not selected. The fixed final state binding energy shows that it originates from the direct double photoionization process:

$$h\nu + \mathrm{Ar} \rightarrow \mathrm{Ar}^{++}2p^{-1}3p^{-1} + e + e(E = 0), \quad (3)$$

where the Ar^{++} states are the same as those populated via the $2s$ hole by Coster-Kronig decay.

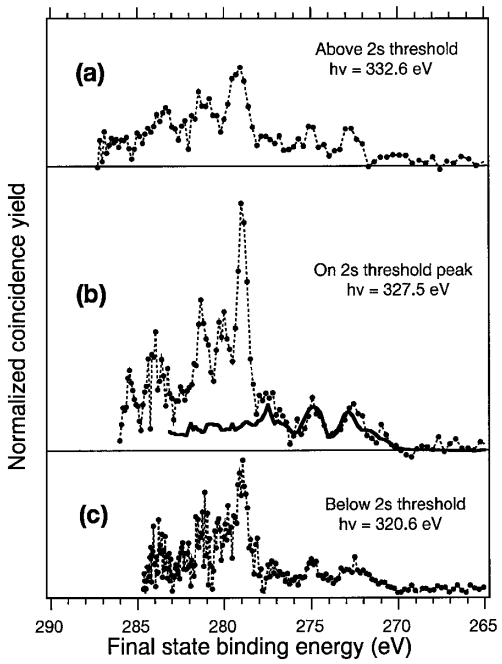

FIG. 3. Coincident spectra taken above (a), below (c), and on (b) the Ar $2s$ threshold peak. The three spectra are plotted on a common intensity scale.

Figure 3 demonstrates that the $2s$ hole leads to an enhancement of the double photoionization cross section to the $Ar^{++}\ 2p^{-1}3p^{-1}$ states that we determined to be by a factor of 3 ± 0.6 on the Ar $2s$ threshold peak. From this result it is clear that, in these experiments, we are, in fact, probing "resonance-affected" double ionization, as defined by Krassig *et al.* [16]. The Auger process formulated in (1) is no more than a resonance in the double ionization continuum represented by process (3). From this standpoint it is obvious that conservation of energy and not intermediate state lifetimes governs the resolution with which one can observe the process.

The well-known limitations of the two-step model of Auger decay appear all the more here, with energy resolutions higher than the lifetime width of the intermediate atomic states. Even in such circumstances, a completely consistent temporal description of our process is possible, as follows: The photoionization process (1) can be described with wave packets [17] of temporal duration $\Delta t = 1/\Delta E$, where $\Delta E = 650$ meV is our total experimental resolution, and our atomic system may stay in a superposition of the states before and after the electron emission for the time duration of Δt, giving the time span of the coherence beyond the atomic lifetime. Our "narrow-band" or "subnatural linewidth" regime, defined by $\Delta E < \Gamma$, implies a temporal length Δt of this wave packet longer than the lifetime of the inner-shell hole, i.e., $\Delta t > \tau = 1/\Gamma$. This means that our experimental time resolution is worse than this lifetime; in other words, our good energy resolution is counterbalanced by an uncertainty in the time of photon absorption Δt that is larger than τ. The emission of the Auger electron also follows this temporal uncertainty, and because of this, energy resolution $\Delta E = 1/\Delta t$ better than the natural width Γ can be attained in the energy of the Auger electron. This shows the inadequacy of a simple two-step model in the case here. One could say, instead, that we are dealing with a "blurred" two-step process.

Analogies between Auger-threshold photoelectron coincidence spectroscopy and resonant Raman Auger spectroscopy [17], i.e., the study of Auger spectra produced by the decay of neutral states with an inner-shell vacancy, must be briefly mentioned. First, the subnatural linewidth regime can be viewed in both cases as a natural consequence of conservation of energy where the inner-shell lifetime plays no part [18]; second, both can be considered resonant processes, with the difference that the intermediate step involves ionization of an inner-shell electron in one case and its excitation in the other. In the terminology of the field of Auger spectroscopy, the present new spectroscopy technique could then be called, "above threshold" or "continuum" resonant Raman Auger spectroscopy.

In summary, the first Coster-Kronig spectrum with subnatural linewidth resolution is presented. This illustrates the power of the Auger-threshold photoelectron coincidence technique in performing high resolution Auger spectroscopy. This technique can also clarify Auger spectra, by filtering out weak components, such as those associated here with Ar $2s$ decay. In the future, as the photon resolution and intensity of beam lines at synchrotrons increases, this technique is expected to help unravel Auger spectra and provide a new spectroscopic tool for the study of doubly charged ions. Further investigation aimed at molecular systems are in preparation and, in addition, are expected to reveal dynamical phenomena analogous to those seen in Auger spectroscopy of neutral states [17].

We are most grateful to Kenji Ito for many fruitful discussions during the course of this work, and acknowledge the support of the SuperACO staff.

[1] J. Viefhaus *et al.*, Phys. Rev. Lett. **80**, 1618 (1998).
[2] W. Mehlhorn, Z. Phys. **201**, 1 (1968).
[3] P. Glans *et al.*, Phys. Rev. A **47**, 1539 (1993).
[4] K. Okuyama *et al.*, Phys. Rev. A **41**, 4930 (1990).
[5] U. Alkemper *et al.*, Phys. Rev. A **56**, 2741 (1997).
[6] K. Lee *et al.*, in *Atomic and Molecular Photoionization*, edited by A. Yagishita and T. Sasaki, (Universal Academy Press, Tokyo, 1996), p. 119.
[7] M. Neeb *et al.*, J. Phys. B **29**, 43 811 (1996).
[8] H. W. Haak *et al.*, Phys. Rev. Lett. **41**, 1825 (1978); for a recent review, see S. M. Thurgate, J. Electron. Spectrosc. Relat. Phenom. **81**, 1 (1996).
[9] F. Penent *et al.*, Phys. Rev. Lett. **81**, 3619 (1998).
[10] S. Cvejanovic and F. H. Read, J. Phys. B **7**, 1180 (1974).
[11] B. Langer *et al.*, J. Phys. B **30**, 593 (1997).
[12] L. Avaldi *et al.*, J. Phys. B **27**, 3953 (1994).
[13] R. Karim and B. Crasemann, Phys. Rev. A **31**, 709 (1985).
[14] W. Mehlhorn, Phys. Lett. **26A**, 166 (1968).
[15] P. Lablanquie *et al.*, *Proceedings of the International Workshop on Photoionization, Chester, UK, Abstracts of Contributed Papers, 1997,* p. 96 (unpublished).
[16] B. Krassig *et al.*, J. Phys. B **26**, 2589 (1993).
[17] S. Sundin *et al.*, Phys. Rev. Lett. **79**, 1451 (1997); O. Bjorneholm *et al.*, Phys. Rev. Lett. **79**, 3150 (1997); M. Simon *et al.*, Phys. Rev. Lett. **79**, 3857 (1997); E. Pahl *et al.*, Phys. Rev. Lett. **80**, 1865 (1998).
[18] T. LeBrun, in *Raman Emission by X-Ray Scattering*, edited by D. L. Ederer and J. H. McGuire (World Scientific, Singapore, 1996), p. 142.